

## Probing Electric and Magnetic Vacuum Fluctuations with Quantum Dots

P. Tighineanu,<sup>\*</sup> M. L. Andersen, A. S. Sørensen, S. Stobbe, and P. Lodahl<sup>†</sup>

*Niels Bohr Institute, University of Copenhagen, Blegdamsvej 17, DK-2100 Copenhagen, Denmark*

(Received 4 April 2014; published 25 July 2014)

The electromagnetic-vacuum-field fluctuations are intimately linked to the process of spontaneous emission of light. Atomic emitters cannot probe electric- and magnetic-field fluctuations simultaneously because electric and magnetic transitions correspond to different selection rules. In this Letter we show that semiconductor quantum dots are fundamentally different and are capable of mediating electric-dipole, magnetic-dipole, and electric-quadrupole transitions on a single electronic resonance. As a consequence, quantum dots can probe electric and magnetic fields simultaneously and can thus be applied for sensing the electromagnetic environment of complex photonic nanostructures. Our study opens the prospect of interfacing quantum dots with optical metamaterials for tailoring the electric and magnetic light-matter interaction at the single-emitter level.

DOI: [10.1103/PhysRevLett.113.043601](https://doi.org/10.1103/PhysRevLett.113.043601)

PACS numbers: 42.50.Ct, 73.20.Mf, 78.67.Hc

Spontaneous emission is a fundamental physical process, which plays an essential role in nature as the main source of optical radiation, and in applications as the principal source of artificial illumination. Quantum mechanically, spontaneous emission is an effect of the fluctuating electromagnetic vacuum field perturbing the emitter. At optical frequencies, emitters sense mainly the electric field while higher-order multipole field components can be neglected. This is because the variation of the electromagnetic field is negligible over the spatial extent of most quantum emitters, which has rendered the dipole approximation a highly successful approximation in quantum electrodynamics. Nevertheless, magnetic-dipole (MD) and electric-quadrupole (EQ) transitions are well known in atomic physics and can be accessed with light despite being much weaker [1–3], since they have different selection rules than electric-dipole (ED) transitions [4–6]. Self-assembled quantum dots (QDs) are fundamentally different and the dipole approximation may not apply to QDs even on dipole-allowed transitions, as was recently found experimentally [7]. The asymmetry of the QD wave functions originating from a lack of mirror-reflection symmetry (parity symmetry) of the QD confinement potential breaks the usual selection rules applicable in atomic physics leading to both ED and multipolar contributions on the same transition. For atoms, a related but very weak asymmetry is induced by the electroweak interaction and has been used to probe the standard model of particle physics [8]. In contrast, the parity violation is very strong for QDs due to their asymmetric structure and, therefore, they may be exploited as a probe of the parity of the photonic nanostructure or the nature of the multipolar quantum-vacuum fluctuations.

In the present work, we show that the commonly used self-assembled In(Ga)As QDs are sensitive to both electric and magnetic fields. The multipolar effects explained by our theory are relevant and important in

many nanophotonic configurations. A current hot topic in nanophotonics exploits the role of nonlocality of the dielectric response in plasmonics [9,10]. Here we study a different nonlocal phenomenon by accounting for the spatial extent and symmetry of QDs and their interaction with the complex field profiles found in nanostructures of importance for photon emission. The effect is particularly pronounced if both the QD and the nanophotonic environment violate parity symmetry. The developed formalism is remarkably simple, as we obtain a single light-matter interaction channel for the multipolar part, which, combined with the usual ED contribution, describes completely the QD-field interaction. For concreteness we consider the QD spontaneous emission for two experimentally realistic nanophotonic structures: a semiconductor-metal plane interface and a plasmonic nanowire [see Fig. 1(a)]. We note that our results apply to self-assembled QDs while, e.g., spherical nanocrystals would not possess the required symmetry. Our study demonstrates that single QDs can be employed for locally probing complex photonic nanostructures that tailor both the electric and magnetic field [11,12]. Sensitivity to the magnetic field has been a long-sought goal in nanophotonics, and has been achieved so far only by scanning near-field spectroscopy [13], where the disturbance of the electromagnetic field profile by the applied near-field probe can be an issue. The nanometer size of single QDs enables noninvasive probing that operates at the single-electron single-photon level.

The present analysis concentrates on the rate of spontaneous emission  $\Gamma$  of the QD because it is a direct and experimentally relevant measure of the light-matter coupling strength [14,15]. Another interesting property would be the emission pattern of the QD that can be modified and tailored by the interference of dipolar and multipolar contributions [3]. In contrast, the multipolar effects discussed here do not affect the QD interaction with phonons, an essential dephasing mechanism, since the

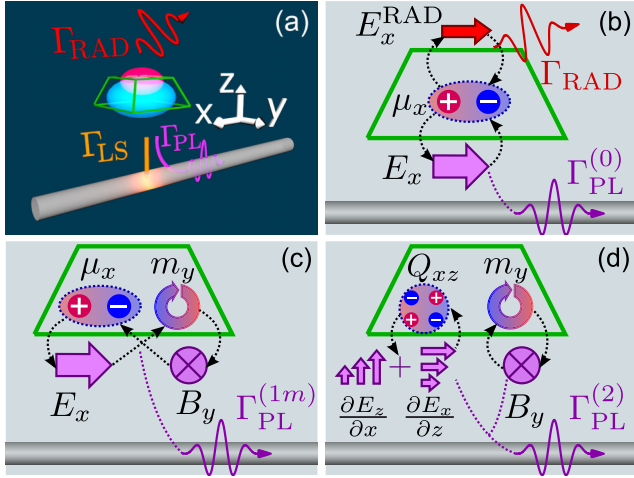


FIG. 1 (color online). Decay dynamics of mesoscopic QDs beyond the dipole approximation. (a) Schematic of the QD decay channels in the proximity of a metal interface. The electron (blue) and hole (red) wave functions illustrate the built-in asymmetry. (b) Light-matter interaction processes governing  $\Gamma^{(0)}$ , where the ED interacts with the radiation modes (RAD) of the electric vacuum  $E_x^{\text{RAD}}$  and the guided surface plasmon (PL) modes  $E_x$ . (c) Processes governing the ED-MD interference. The light emitted by the ED  $\mu_x$  interacts with the MD  $m_y$  and creates a magnetic field. The physical picture of  $\Gamma^{(1Q)}$  is conceptually analogous. (d) Processes governing  $\Gamma^{(2)}$  with pure MD and EQ contributions. The EQ  $Q_{xz}$  couples to the gradient of the electric vacuum.

interaction depends mainly on the QD volume rather than symmetry. We emphasize that the developed theory can readily be extended to cover the strong-coupling regime because the multipolar terms enter as a renormalization of the light-matter coupling strength. Since the coupling strength depends on the interference of multipolar terms as determined by the nanostructure, one may envision designing special nanocavities in order to enhance the light-matter interaction beyond that of a point dipole with immediate applications to quantum light sources for quantum-information processing [16]. It should be mentioned that the mesoscopic terms do not influence the photon statistics of the source, i.e., the excellent single-photon purity observed for QD sources prevails also under conditions where mesoscopic contributions are significant.

According to Fermi's golden rule [17],  $\Gamma = (\pi/\epsilon_0\hbar\omega) \times \sum_l |T_l|^2 \delta(\omega - \omega_l)$ , where the generalized Coulomb gauge [18] is applied,  $T_l = (e/m_0) \langle \Psi_g | \mathbf{f}_l^*(\mathbf{r}) \cdot \hat{\mathbf{p}} | \Psi_e \rangle$  is the transition moment between the ground  $|\Psi_g\rangle$  and excited  $|\Psi_e\rangle$  electronic states of the QD,  $\hat{\mathbf{p}} = -i\hbar\nabla$  the momentum operator,  $\mathbf{f}_l$  the normal vector-potential mode [19], and  $e$  and  $m_0$  the elementary charge and electron mass. At this point, the standard textbook approach is to invoke the dipole approximation  $\mathbf{f}_l(\mathbf{r}) \approx \mathbf{f}_l(\mathbf{r}_0)$  by assuming that the field varies slowly over the QD ( $L_{\text{QD}}$ ), i.e.,  $kL_{\text{QD}} \ll 1$ , where  $k$  is the photon wave number and  $\mathbf{r}_0$  the position of the QD. We account for the field varying over the QD and perform a Taylor expansion in the field modes  $\mathbf{f}_l(\mathbf{r})$ . The expansion can be

performed as long as  $kL_{\text{QD}} < 1$ , otherwise, the integration in  $\Gamma$  must be evaluated directly [20], thereby complicating the analysis and offering limited physical insight [21,22]. The expansion is inserted into the transition moment  $T_l = T_l^{(0)} + T_l^{(1)} + T_l^{(2)} + \dots$ , which yields

$$T_l = \mu_i f_{l,i}^*(0) + \Lambda_{ji} \partial_j f_{l,i}^*(0) + \Omega_{kji} \partial_j \partial_k f_{l,i}^*(0) + \dots, \quad (1)$$

where the summation convention over repeated indices and  $\mathbf{r}_0 = 0$  are used. Here,  $\mu_i = (e/m_0) \langle \Psi_g | \hat{p}_i | \Psi_e \rangle$ ,  $\Lambda_{ij} = (e/m_0) \langle \Psi_g | x_i \hat{p}_j | \Psi_e \rangle$ , and  $\Omega_{ijk} = (e/2m_0) \langle \Psi_g | x_i x_j \hat{p}_k | \Psi_e \rangle$  are the dipole moment, first-order, and second-order mesoscopic moments of the QD, respectively. In the Supplemental Material [23] we show that the contribution from  $\Omega$  is negligible, and  $\boldsymbol{\mu}$  and  $\boldsymbol{\Lambda}$  have the form

$$\boldsymbol{\mu} = \mu \hat{\mathbf{x}}, \quad \boldsymbol{\Lambda} = \Lambda \hat{\mathbf{x}} \hat{\mathbf{z}}, \quad (2)$$

where  $\mu \equiv \mu_x$  and  $\Lambda \equiv \Lambda_{xz}$ . Remarkably, one single parameter  $\Lambda$  describes the light-matter interaction beyond the dipole approximation. The ratio  $|\Lambda/\mu|$  quantifies the mesoscopic strength of the QD and was measured to be about 10 nm for standard self-assembled In(Ga)As QDs [7]. This value will be used throughout the Letter. The interaction with light can be either suppressed or enhanced by the mesoscopic moment  $\Lambda$  depending on the properties of the environment of the QD. This effect is illustrated in Fig. 2(a), where the emission rate of a QD in the proximity of a silver interface is shown (at an emission wavelength of 1000 nm and with the refractive indices of GaAs  $n_{\text{GaAs}} = 3.42$  and of silver  $n_{\text{Ag}} = 0.2 + 7i$ ). A QD and a point dipole exhibit different functional dependencies to the metal interface because the former couples also to field gradients while the latter does not, as is shown in the following. Note that, unlike QDs, atomic wave functions possess parity symmetry so that  $\boldsymbol{\mu}$  and  $\boldsymbol{\Lambda}$  never contribute simultaneously.

We similarly collect the orders in the decay rate as  $\Gamma \approx \Gamma^{(0)} + \Gamma^{(1)} + \Gamma^{(2)}$ . In the proximity of metals, the QD can decay into propagating photons with the rate  $\Gamma_{\text{RAD}}$ , propagating surface plasmons ( $\Gamma_{\text{PL}}$ ), or Ohmic-lossy modes (LS) in the metal ( $\Gamma_{\text{LS}}$ ) [24]; see Fig. 1(a). The former coupling to radiative modes is essentially not affected by multipolar effects since the responsible electromagnetic field varies weakly in space, i.e.,  $\Gamma_{\text{RAD}} \approx \Gamma_{\text{RAD}}^{(0)}$ . In contrast, the plasmon field varies strongly and therefore multipolar effects influence the excitation rate of plasmons. The coupling to lossy modes is normally negligible for distances larger than  $\sim 20$  nm from the metal and we do not discuss them further. We thus obtain the three light-matter interaction channels for mesoscopic QDs,

$$\begin{aligned} \Gamma^{(0)} &= A |\mu|^2 \text{Im}\{G_{xx}(0, 0)\} = \Gamma_{\text{RAD}} + \Gamma_{\text{PL}}^{(0)}, \\ \Gamma^{(1)} &= 2A \text{Re}(\Lambda \mu^*) \partial_x \text{Im}\{G_{zx}(\mathbf{r}, 0)\}|_{\mathbf{r}=0} \approx \Gamma_{\text{PL}}^{(1)}, \\ \Gamma^{(2)} &= A |\Lambda|^2 \partial_x \partial_x' \text{Im}\{G_{zz}(\mathbf{r}, \mathbf{r}')\}|_{\mathbf{r}=\mathbf{r}'=0} \approx \Gamma_{\text{PL}}^{(2)}, \end{aligned} \quad (3)$$

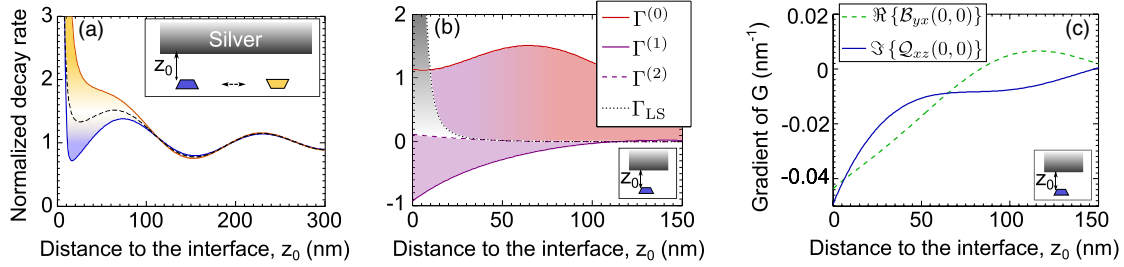


FIG. 2 (color online). Decay dynamics of QDs near a silver interface. All the rates are normalized to the decay rate in homogeneous GaAs. (a) Decay rate for the direct (inverted) QD orientation marked by blue (orange) lines. The black dashed line denotes the dipole theory. (b) Decomposition of the decay rates according to the expansion order. The Ohmic losses are indicated by the dotted black line. (c) The ED-MD and ED-EQ Green's tensor probed by mesoscopic QDs and normalized to  $\text{Im}\{G_{xx}(0,0)\}$  in homogeneous GaAs.

where  $A = 2e^2/\epsilon_0\hbar m_0^2 c_0^2$ ,  $c_0$  is the vacuum speed of light,  $\mathbf{G}(\mathbf{r}, \mathbf{r}')$  the electromagnetic Green's tensor [25], and  $\text{Re}$  and  $\text{Im}$  denote the real- and imaginary-part operators, respectively. Each order has a clear physical meaning as explained below, where we exemplify a semiconductor-silver interface as sketched in the inset of Fig. 2(a).

The zeroth-order rate  $\Gamma^{(0)}$  is the well-known ED contribution, and is given as a product of a field term,  $\text{Im}\{G_{xx}\}$ , which is proportional to the (electric) local density of optical states, and a QD term  $|\mu|^2$ , which is proportional to the (electric) oscillator strength [19]. Here, a microscopic polarization in the  $x$  direction couples to the  $x$ -polarized electric field, which probes the environment and interferes back with itself. The resulting field excitation propagates away from the QD in the form of free photons or surface plasmons; see Fig. 1(b). In the proximity of an interface,  $\Gamma^{(0)}$  has the well-known Drexhage dependence [26]; see Figs. 2(a) and 2(b), where the red-violet color gradient indicates that the coupling to the plasmonic field becomes dominant at distances smaller than  $\sim 50$  nm.

The higher-order corrections to  $\Gamma$  depend on the mesoscopic moment  $\Lambda$ , which is responsible for the nonlocal interaction with light.  $\Gamma^{(1)}$  is a first-order process and is negligible if the figure of merit  $\mathcal{G}^{(1)} \equiv |\Gamma^{(1)}|/\Gamma^{(0)} \approx k \times 2|\Lambda/\mu|$  is much smaller than unity. For In(Ga)As QDs,  $\mathcal{G}^{(1)} \approx 0.44$  shows that the light-matter interaction beyond the dipole approximation can be strong. The magnitude of such effects is determined by the field gradients of the particular photonic nanostructure and we compute them in the next paragraph.  $\Gamma^{(2)}$  is a second-order process and contains pure MD and EQ contributions as sketched in Fig. 1(d). For QDs, the important quantity is  $\mathcal{G}^{(2)} \equiv |\Gamma^{(2)}|/\Gamma^{(0)} \approx k^2|\Lambda/\mu|^2 \approx 0.05$ , which is negligible. Note that the dipole approximation is more robust for atoms and other high-symmetry emitters, since the first nonvanishing contribution is  $\Gamma^{(2)}$ , which has a weight of  $(kL_{\text{QD}})^2$  with respect to  $\Gamma^{(0)}$ .

In the following, we discuss the first-order contribution  $\Gamma^{(1)}$  in quantitative terms. The mesoscopic moment  $\Lambda$  contains MD and EQ contributions, as can be seen from

$$\Lambda_{xz}\partial_x e_{l,z}(0) = i\omega m_y b_{l,y}(0) + Q_{xz}[\partial_x e_{l,z}(0) + \partial_z e_{l,x}(0)], \quad (4)$$

where  $\mathbf{e}$  and  $\mathbf{b}$  are the electric- and magnetic-field modes, respectively,  $m_y \equiv m$  the MD and  $Q_{xz} \equiv Q$  the EQ of the QD [27]. The two moments are equal, i.e.,  $m = Q = \Lambda/2$ , but they couple to different field components and thus their contribution can be tailored independently. As a consequence,  $\Gamma^{(1)}$  intertwines the ED, MD, and EQ characters of the QD with the following physical interpretation. The ED couples to the  $x$ -polarized electric field, which probes the environment and interferes back with the MD and EQ components; see Fig. 1(c). The resulting field excitation propagates away in the form of surface plasmons. Note that  $\Gamma^{(1)} \neq 0$  only if both the QD wave functions and the electromagnetic environment violate parity symmetry. This is because a parity-symmetric electronic potential cannot be both  $\mu$  and  $\Lambda$  allowed, and a parity-symmetric environment contains either even or odd electromagnetic modes. The ED is an even operator and would couple only to the even modes, while  $\Lambda$  corresponds to an odd operator and would couple to the odd modes inducing no mutual interference between  $\mu$  and  $\Lambda$  and a vanishing  $\Gamma^{(1)}$ . The first-order contribution can both enhance and suppress the light-matter interaction depending on whether the light emitted by the ED  $\mu$  interferes constructively or destructively with the mesoscopic moment  $\Lambda$ . This can be seen in Fig. 2(a), where by flipping the QD orientation  $\Lambda$  changes sign and, hence,  $\Gamma^{(1)}$  changes from suppressing to enhancing the decay rate. The multipolar contribution to  $\Gamma^{(1)}$  is

$$\begin{aligned} \Gamma^{(1)} &= \Gamma^{(1m)} + \Gamma^{(1Q)} \\ &= A\omega m_y \mu^* \text{Re}\{\mathcal{B}_{yx}(0,0)\} + A Q_{xz} \mu^* \text{Im}\{\mathcal{Q}_{xz}(0,0)\}, \end{aligned} \quad (5)$$

where we define the ED-MD Green's tensor  $\mathcal{B}_{yx}(0,0) = -i\omega^{-1}[\partial_x G_{zx}(\mathbf{r},0) - \partial_z G_{xx}(\mathbf{r},0)]_{\mathbf{r}=\mathbf{0}}$ , the ED-EQ Green's tensor  $\mathcal{Q}_{xz}(0,0) = [\partial_x G_{zx}(\mathbf{r},0) + \partial_z G_{xx}(\mathbf{r},0)]_{\mathbf{r}=\mathbf{0}}$ , and assume  $\Lambda\mu^*$  to be real [28]. Equation (5) shows that QDs access the magnetic and electric-quadrupole vacuum

fields and is demonstrated in Fig. 2(c), where the contribution of  $\text{Re}\{\mathcal{B}_{yx}(0,0)\}$  and  $\text{Im}\{\mathcal{Q}_{xz}(0,0)\}$  is shown. The two components of the Green's tensor vary over length scales of tens of nanometers, which is comparable to the QD size [29] and explains the breakdown of the dipole approximation observed in experiment [7].

QDs interact with light as spatially extended objects and are, therefore, capable of probing not only the electric-field magnitude at their position but also field variations. This is the basic property allowing us to use QDs for probing the electromagnetic vacuum fluctuations. If placed in an unknown nanophotonic structure, the spontaneous-emission rate of the QD is generally given by  $\Gamma_{\uparrow} \approx \Gamma_{\uparrow}^{(0)} + \Gamma_{\uparrow}^{(1)}$ . By flipping the QD orientation, which is a feasible experimental procedure that can be done by etching away the substrate [7], the ED contribution is the same but the first-order term changes sign, i.e.,  $\Gamma_{\downarrow} \approx \Gamma_{\downarrow}^{(0)} + \Gamma_{\downarrow}^{(1)} = \Gamma_{\uparrow}^{(0)} - \Gamma_{\uparrow}^{(1)}$ . As a consequence, both the projected Green's tensor  $\text{Im}\{G_{xx}(0,0)\}$  and the spatial gradient  $\partial_x \text{Im}\{G_{zx}(0,0)\}$  can be unambiguously extracted; cf. Eq. (3). While the former corresponds to the electric-field strength generated by an ED at the position of the emitter, the latter describes the electric-field gradient generated by the same ED. We exemplify this aspect by investigating the interaction between QDs and surface plasmons in the proximity of a silver nanowire (radius  $\rho = 30$  nm), which is capable of collecting most of the QD emission into a single propagating field mode, an important goal in the field of quantum photonics [16,30]. We find the nanowire to support a single strongly confined plasmon mode with  $\mathcal{G}^{(1)} = k_{\text{PL}} \times 2|\Lambda/\mu| = 0.76$  [19,30] leading to stronger field gradients than for the plane silver interface. The contribution of  $\Gamma^{(2)}$  is again negligible since  $\mathcal{G}^{(2)} = 0.14$ . The coupling to radiation and lossy modes is modeled as a point dipole in the simple quasistatic approximation [30,31], which gives excellent agreement with the electrodynamic computation [32]. The Green's tensor of the plasmon field acquires a particularly simple form [32] and for the geometry presented in Fig. 3(a) the relevant rates read

$$\frac{\Gamma_{\text{PL}}^{(0)}}{\Gamma_{\text{GaAs}}^{(0)}} = C|e_z(0)|^2, \quad (6)$$

$$\frac{\Gamma_{\text{PL}}^{(1)}}{\Gamma_{\text{GaAs}}^{(0)}} = 2C \frac{\Lambda}{\mu} \text{Re}\{[\partial_z e_r^*(0)]e_z(0)\}, \quad (7)$$

where  $C = 3\pi c_0 \epsilon_0 / nk_0^2 v_g$ ,  $v_g$  is the group velocity of the guided mode, and the decay rates have been normalized to the decay rate in homogeneous GaAs. Equations (6)–(7) contain the two field components, which can be probed by QDs in spontaneous-emission experiments, as shown in the following.

There are two configurations in which the plasmon density of optical states is nonzero, namely, for an axially and radially oriented dipole [30]; see the inset of Figs. 3(a), 3(d). If the dipole moment is oriented axially, cf. Fig. 3(a),

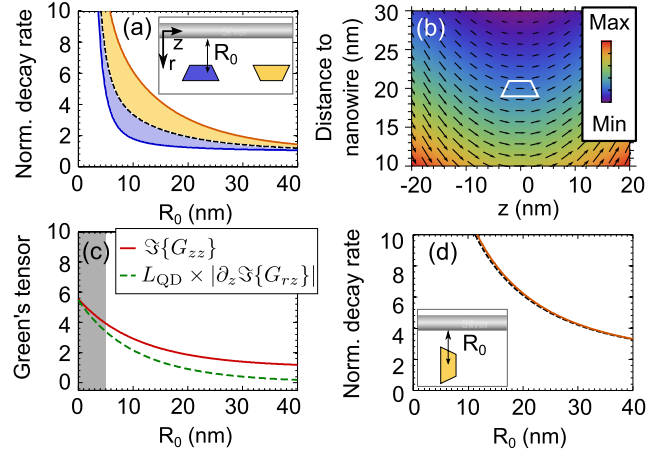


FIG. 3 (color online). Probing field gradients with mesoscopic QDs. (a) For an axially oriented dipole,  $\Gamma^{(1)}$  enhances (suppresses) the light-matter interaction for the configuration marked by orange (blue). The dashed line is the prediction of the dipole theory. (b) Vector plot of the plasmonic field generated by the ED of the QD situated 20 nm away from the nanowire. Both the length of the arrows and the color scale denote the field magnitude. (c) The field projections probed by the QD can be extracted by subtracting the decay curves in (a). The gray-shaded area is the region where nonradiative losses are dominant. (d) For a radially oriented dipole,  $\Gamma^{(1)} = 0$  and the QD behaves as an electric dipole.

we find the coupling to surface plasmons to be suppressed completely when  $\Lambda$  and  $\mu$  are in phase [ $\Lambda/\mu > 0$ , depicted with blue in Fig. 3(a)] and enhanced by a factor of 2 when they are  $\pi$  out of phase ( $\Lambda/\mu < 0$ , depicted with orange). Using the aforementioned procedure of recording  $\Gamma_{\uparrow}$  and  $\Gamma_{\downarrow}$  from Fig. 3(a), QDs can be used to probe the magnitude and curvature of the complex plasmonic field plotted in Fig. 3(b). At the center of the QD, the field is completely polarized along the  $z$  direction and the point-dipole character of the QD therefore probes the local density of states via  $\text{Im}\{G_{zz}(0,0)\}$ . Additionally, the field exhibits a curvature meaning that the radially polarized field varies over the QD despite the fact that its mean value is zero. This radially polarized axial gradient,  $\partial_z \text{Im}\{G_{rz}(\mathbf{r},0)\}$ , is probed by the extended mesoscopic character of the QD. Both fields exhibit a monotonic increase as the QD approaches the nanowire and are plotted in Fig. 3(c). The axial gradient is multiplied by the in-plane QD size ( $L_{\text{QD}} = 20$  nm) [29] to show the field variation over the QD spatial extent. It is interesting to note that the field  $\text{Im}\{G_{rz}\}$  exhibits a large variation over the QD that is comparable to the probed field itself  $\text{Im}\{G_{zz}\}$ . This example shows the “ease” of breaking the dipole approximation with QDs in nanophotonic structures. We find that most of the contribution to  $\Gamma_{\text{PL}}^{(1)}$  stems from the EQ nature of the QD, in contrast to the silver interface, where the MD and EQ contributions are of comparable magnitude. These examples show that even though the MD and EQ moments are equal in magnitude, their individual contribution to the

light-matter interaction can be tailored by correspondingly engineering the nanophotonic environment. In this sense, QDs are promising light emitters for embedment in optical metamaterials, whose practical realization has become technologically feasible over the past years. In the second configuration, the dipole moment is oriented radially and the first-order contribution  $\Gamma^{(1)}$  vanishes because the environment is parity symmetric along the QD height; see the inset of Fig. 3(d). Consequently, the QD probes only the local density of optical states and the dipole approximation is a very good assumption. As seen in Fig. 3(d), the prediction of the two theories are very close.

In conclusion, we have shown that the commonly employed In(Ga)As QDs are capable of strongly interacting with the multipolar quantum vacuum on dipole-allowed transitions. This striking behavior is triggered by the lack of parity symmetry of the electronic wave functions and of the electromagnetic environment. The effect can be exploited to use QDs as a probe of the local field environment revealing not only information about the field itself but also about its gradients. Furthermore, by engineering the nanophotonic environment it is possible to selectively access the MD or EQ nature of the QD and, thereby, to tailor the multipolar radiation of semiconductor QDs. We have exemplified this for metal nanostructures but any strongly or rapidly varying optical modes would produce deviations from the dipole approximation, and we therefore expect this work to be of significance not only for plasmon-based devices [33] and photovoltaics [34], but also for the active field of photonic-crystal cavities and waveguides, where QDs have been described as dipole emitters so far.

We thank P. T. Kristensen for valuable discussions. We gratefully acknowledge the financial support from the Danish Council for Independent Research (natural sciences and technology and production sciences), the European Research Council (ERC consolidator grants ALLQUANTUM and QIOS), and the Carlsberg Foundation.

\*petru.tighineanu@nbi.ku.dk

†lodahl@nbi.ku.dk

- [1] M. C. Noecker, B. P. Masterson, and C. Wieman, *Phys. Rev. Lett.* **61**, 310 (1988).
- [2] I. D. Rukhlenko, D. Handapangoda, M. Premaratne, A. V. Fedorov, A. V. Baranov, and C. Jagadish, *Opt. Express* **17**, 17570 (2009).
- [3] T. H. Taminiau, S. Karaveli, N. F. van Hulst, and R. Zia, *Nat. Commun.* **3**, 979 (2012).
- [4] J. R. Zurita-Sánchez and L. Novotny, *J. Opt. Soc. Am. B* **19**, 1355 (2002).
- [5] J. R. Zurita-Sánchez and L. Novotny, *J. Opt. Soc. Am. B* **19**, 2722 (2002).
- [6] G. Y. Slepyan, A. Magyarov, S. A. Maksimenko, and A. Hoffmann, *Phys. Rev. B* **76**, 195328 (2007).
- [7] M. L. Andersen, S. Stobbe, A. S. Sørensen, and P. Lodahl, *Nat. Phys.* **7**, 215 (2011).
- [8] C. Wood, S. Bennett, D. Cho, B. Masterson, J. Roberts, C. Tanner, and C. Wieman, *Science* **275**, 1759 (1997).
- [9] C. Ciraci, R. Hill, J. Mock, Y. Urzhumov, A. Fernández-Domínguez, S. Maier, J. Pendry, A. Chilkoti, and D. Smith, *Science* **337**, 1072 (2012).
- [10] G. Toscano, S. Raza, W. Yan, C. Jeppesen, S. Xiao, M. Wubs, A.-P. Jauho, S. I. Bozhevolnyi, and N. A. Mortensen, *Nanophotonics* **2**, 161 (2013).
- [11] C. M. Soukoulis and M. Wegener, *Science* **330**, 1633 (2010).
- [12] J. B. Pendry, D. Schurig, and D. R. Smith, *Science* **312**, 1780 (2006).
- [13] M. Burrelli, D. Van Oosten, T. Kampfrath, H. Schoenmaker, R. Heideman, A. Leinse, and L. Kuipers, *Science* **326**, 550 (2009).
- [14] Q. Wang, S. Stobbe, and P. Lodahl, *Phys. Rev. Lett.* **107**, 167404 (2011).
- [15] P. Tighineanu, R. Daveau, E. H. Lee, J. D. Song, S. Stobbe, and P. Lodahl, *Phys. Rev. B* **88**, 155320 (2013).
- [16] P. Lodahl, S. Mahmoodian, and S. Stobbe, *arXiv:1312.1079*.
- [17] C. Cohen-Tannoudji, B. Diu, and F. Laloë, *Quantum Mechanics*, Vol. 2 (John Wiley & Sons, New York, 2005).
- [18] N. Vats, S. John, and K. Busch, *Phys. Rev. A* **65**, 043808 (2002).
- [19] L. Novotny and B. Hecht, *Principles of Nano-Optics* (Cambridge University Press, Cambridge, England, 2012).
- [20] K. Jun Ahn and A. Knorr, *Phys. Rev. B* **68**, 161307 (2003).
- [21] S. Stobbe, P. T. Kristensen, J. E. Mortensen, J. M. Hvam, J. Mørk, and P. Lodahl, *Phys. Rev. B* **86**, 085304 (2012).
- [22] P. T. Kristensen, J. E. Mortensen, P. Lodahl, and S. Stobbe, *Phys. Rev. B* **88**, 205308 (2013).
- [23] See Supplemental Material at <http://link.aps.org/supplemental/10.1103/PhysRevLett.113.043601> for the entries of the first- ( $\mathbf{A}$ ) and second-order ( $\mathbf{\Omega}$ ) mesoscopic moments of QDs using simple arguments based on parity symmetry.
- [24] J. Kalkman, H. Gersen, L. Kuipers, and A. Polman, *Phys. Rev. B* **73**, 075317 (2006).
- [25] M. Paulus, P. Gay-Balmaz, and O. J. F. Martin, *Phys. Rev. E* **62**, 5797 (2000).
- [26] K. Drexhage, *J. Lumin.* **1**, 693 (1970).
- [27] S. Bernadotte, A. J. Atkins, and C. R. Jacob, *J. Chem. Phys.* **137**, 204106 (2012).
- [28] P. Tighineanu, A. S. Sørensen, S. Stobbe, and P. Lodahl (to be published).
- [29] D. Bruls, J. Vugs, P. Koenraad, H. Salemink, J. Wolter, M. Hopkinson, M. Skolnick, F. Long, and S. Gill, *Appl. Phys. Lett.* **81**, 1708 (2002).
- [30] D. E. Chang, A. S. Sørensen, P. R. Hemmer, and M. D. Lukin, *Phys. Rev. B* **76**, 035420 (2007).
- [31] V. V. Klimov and M. Ducloy, *Phys. Rev. A* **69**, 013812 (2004).
- [32] Y. Chen, T. R. Nielsen, N. Gregersen, P. Lodahl, and J. Mørk, *Phys. Rev. B* **81**, 125431 (2010).
- [33] J. A. Schuller, E. S. Barnard, W. Cai, Y. C. Jun, J. S. White, and M. L. Brongersma, *Nat. Mater.* **9**, 193 (2010).
- [34] H. A. Atwater and A. Polman, *Nat. Mater.* **9**, 205 (2010).